



HAL
open science

Optimal impedance calculation with a two-measurement MPPT algorithm for piezoelectric vibration harvesters

Nicolas Decroix, Pierre Gasnier, Adrien Badel

► To cite this version:

Nicolas Decroix, Pierre Gasnier, Adrien Badel. Optimal impedance calculation with a two-measurement MPPT algorithm for piezoelectric vibration harvesters. Power-MEMS 22 - The 21st International Conference on Micro and Nanotechnology for Power Generation and Energy Conversion Applications, Dec 2022, Salt Lake City, United States. pp.62-65, 10.1109/Power-MEMS56853.2022.10007581 . cea-04226845

HAL Id: cea-04226845

<https://cea.hal.science/cea-04226845>

Submitted on 3 Oct 2023

HAL is a multi-disciplinary open access archive for the deposit and dissemination of scientific research documents, whether they are published or not. The documents may come from teaching and research institutions in France or abroad, or from public or private research centers.

L'archive ouverte pluridisciplinaire **HAL**, est destinée au dépôt et à la diffusion de documents scientifiques de niveau recherche, publiés ou non, émanant des établissements d'enseignement et de recherche français ou étrangers, des laboratoires publics ou privés.

OPTIMAL IMPEDANCE CALCULATION WITH A TWO-MEASUREMENT MPPT ALGORITHM FOR PIEZOELECTRIC VIBRATION HARVESTERS

Nicolas Decroix^{1,2}, Pierre Gasnier¹, Adrien Morel², David Gibus² and Adrien Badel²

¹Univ. Grenoble Alpes, CEA-LETI, Grenoble, FRANCE and

²Univ. Savoie Mont Blanc, SYMME, Annecy, FRANCE

ABSTRACT

This paper proposes a novel Maximum Power Point Tracking (MPPT) architecture for weakly and highly coupled vibration piezoelectric harvesters. At a given input frequency, the microcontroller-based architecture allows to calculate the optimal impedance by means of voltage and phase measurements. It implements the full-bridge load adaptation technique with a flyback converter, which generates the appropriate optimal resistive load right after the impedance calculation. We proposed a dedicated test-bench with a highly coupled piezoelectric harvester ($k_m^2 = 4.7\%$) to prove and validate the operation of the system. The optimal load was found on the useful frequency range (23.7 Hz - 26 Hz) around the harvester's resonant frequency ($f_{sc} = 24.6$ Hz). The system reached more than 90% of the maximum harvestable power ($P_{max} = 193 \mu\text{W}$ @ 0.2 m/s²). We also proved that the proposed architecture is low power thanks to a low-level programming of the microcontroller: the STM32L4 consumes around 22 μW @ 1.8 V during the emulation of the optimal resistive load.

KEYWORDS

Maximum Power Point Tracking Algorithm – Piezoelectric Energy Harvesting – Microcontroller – Power Management Circuit

INTRODUCTION

Vibration energy harvesting is a promising candidate for powering wireless sensor nodes for IoT. However, the power output of these harvesters heavily depends on the input mechanical conditions (vibration amplitude and frequency) as well as the harvester's unavoidable variations due to its aging or temperature. Piezoelectric Energy Harvesters (PEH) can be classified as strongly or weakly coupled depending on their ability to improve the power extraction bandwidth. In order to harvest power for multiple input conditions, efficient and adaptive Maximum Power Point Tracking (MPPT) algorithms and extraction techniques still need to be implemented.

Recent work have shown that non-linear extraction techniques like SCSECE [1,2] or FTSECE [1,3] greatly improve the harvestable power bandwidth of the PEH. Nevertheless, those techniques have the disadvantage of exciting the higher bending modes of the piezoelectric cantilever, leading to several power drops in the harvesting bandwidth [4]. In this work, the full-bridge two-stage load adaptation technique [1,5], denoted "resistive technique" in this work for compactness, is used. Indeed, this technique is easy to implement and strongly reduces the excitation of the upper modes since the load seen by the PEH during the extraction phases is mostly linear.

There exists several MPPT algorithms regarding piezoelectric energy harvesting. Lookup tables (LUT) for

example uses pre-stored parameters depending on input conditions [6]. This algorithm is not robust to the PEH parameters variations. Perturb & Observe (P&O) algorithm tend to take time to converge to the MPP [7,8]. Half-open circuit voltage (HOCV) algorithms find only an optimal voltage and it is thus not robust to vibration amplitude variation [9]. We propose here an algorithm that is robust to vibration amplitude, frequency and to PEH parameters variation. It calculates the optimal impedance after two successive measurement during a few mechanical periods. Once the optimal impedance is found. It is emulated for a fixed duration until a new measurement is performed. This algorithm is based on [10] and is similar to the one in [11] but the latter only finds the optimal resistive load and not the optimal impedance.

In this paper, we propose and experimentally validate the operation of a novel MCU-based MPPT architecture implementing the resistive extraction technique to perform an optimal resistive matching for piezoelectric vibration harvesters.

EXTRACTION CIRCUIT AND MPPT METHOD

The proposed architecture and its associated test-bench are depicted in Fig. 1. The resistive technique, rarely used in the context of strongly coupled PEH, is similar to the SEH technique but without filter capacitor. Similarly to [5], we use a flyback converter in Discontinuous Current Mode (DCM) downstream of the full-bridge rectifier to emulate the desired resistive load. In this work, the algorithm that we use relies on the fact that the applied load is linear so the resistive technique is well suited for this algorithm.

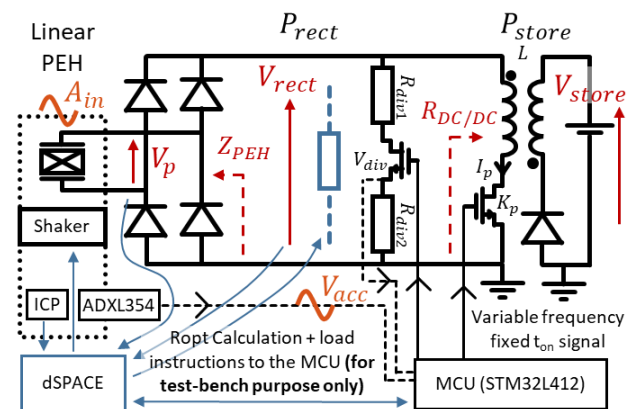


Figure 1 : Architecture of the MPPT method

Our algorithm searches for the optimal impedance by emulating two different resistive loads (two operating points) with the flyback while measuring the phase shift between the ambient acceleration A_{in} and the piezoelectric

voltage V_p . The different steps required to calculate the optimal resistive load R_{opt} are depicted in Fig. 2. In this graph, R_1 and R_2 are the two successive loads emulated by the flyback.

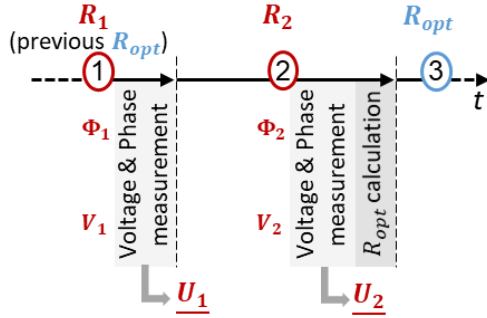


Figure 2 : Temporal description of the MPPT (not scaled)

As described in [10], the two-operating points measurement method allows to obtain the optimal complex impedance of the generator Z_{PEH} (see Fig. 1). In this paper, the system only emulates the optimal resistive load R_{opt} with the DC/DC converter, complex impedance matching being out of the scope of this paper and will be studied in future work. The magnitude of the complex optimal impedance R_{opt} , is then given by Eq. (1) and (2) :

$$R_{opt} = |Z_{PEH}| \quad Z_{PEH} = \frac{(U_2 - U_1) R_1 R_2}{(U_1 R_2 - U_2 R_1)} \quad (1)$$

$$\begin{cases} U_1 = V_1 e^{j\phi_1} \\ U_2 = V_2 e^{j\phi_2} \end{cases} \quad (2)$$

In practice, the system will keep on emulating the previous emulated optimal resistive load R_{opt} to perform the first voltage/phase measurement R_1 (see Fig. 2). Once the system has found the optimal resistive load, the new optimal resistive load one is emulated for a fixed duration until a new measurement cycle is performed.

Thanks to this proposition, only voltage and phase measurements are necessary to perform the optimal load measurement. Measuring voltages and phases is an interesting way of obtaining the generator's impedance as compared with current measurements which often lead to a more complex implementation and a higher power consumption of the electronics. Furthermore, this MPPT architecture, associated with its extraction circuit allows to measure the optimal impedance while extracting the electrical power from the PEH in an efficient and low power way.

Because the accelerometer has to be activated, one can mention that the system consumption will be higher during the measurement steps compared to the load emulation steps. This can be limited by bounding the measurement steps to a few mechanical periods.

IMPLEMENTATION

Our system is based on a microcontroller or MCU (STM321412) surrounded by discrete electronics and an accelerometer. The resistive loads R_1 and R_2 are emulated thanks to the flyback converter (with coupled inductance

RN216-1-01-10M) in DCM. The emulated resistance $R_{DC/DC}$ is given by Eq. (3) :

$$R_{DC/DC} = \frac{2L}{f_{DC/DC} t_{on}^2} \quad (3)$$

With L the inductance value, $f_{DC/DC}$ the frequency of the PWM, and t_{on} the duration of the PWM pulse.

The MCU emulates the loads thanks to a fixed t_{on} pulse signal created with its internal low-power timers fed by a low-power 100 kHz external clock (ref. OM-0100-C8, $\approx 2 \mu A$). Load emulation is active when the MCU is in "Stop 2 mode", which is the lowest power mode of the STM3214 with active low-power timers.

Phase measurement

The phase information is obtained with two zero-crossing detectors based on ultra-low-power comparators (ref. TS881, $\approx 300 nA$). One is used to sense the piezoelectric voltage V_p and the other senses the output of a low-power analog accelerometer (ref. ADXL354, 150 μA) with a high pass filter to remove its offset voltage, as shown in Fig. 3 :

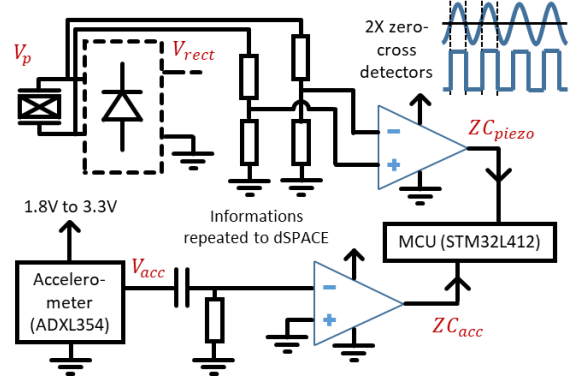


Figure 3 : Phase shift measurement between V_p and V_{acc}

The phase difference between V_p and V_{acc} is calculated with a single timer : it measures the frequency and the time difference between the outputs of the two comparators ZC_{piezo} and ZC_{acc} . The piezoelectric voltage is reduced thanks to 4 resistors, to be compatible with the voltage supply of the comparators (1.8V to 3.3V).

Voltage measurement

We need here to measure the voltage output of the PEH before the flyback converter at V_{rect} . As there is no low impedance path between the diode bridge and the flyback converter, a part of the non-transferred energy (leakage inductance of the flyback) is locked up in parasitic capacitors (Diodes, MOSFET, ..). Therefore, a periodic measurement of the voltage V_{rect} could lead to false voltage measurements and a wrong estimation of the optimal impedance (see Fig 4 and 5). We propose here to measure V_{rect} only during the first conduction stage of the flyback converter, i.e when K_p is turned-on. This way, the measured voltage V_{rect} is equal to the piezoelectric voltage V_p minus two times the diode threshold voltage. One can note that, the sampling frequency now depends on the operating frequency of the flyback converter $f_{DC/DC}$.

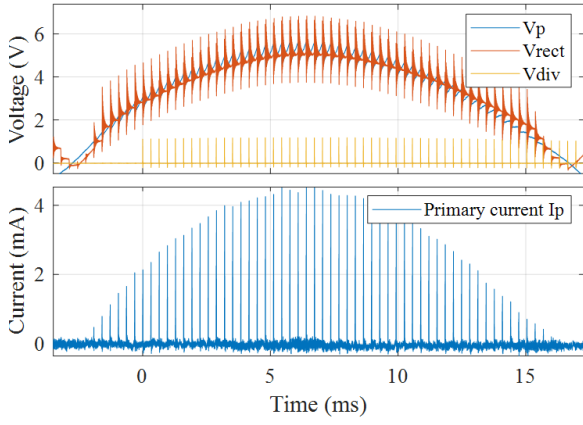


Figure 4 : Voltage and current measurements during half a mechanical period when the DC/DC converter is operating

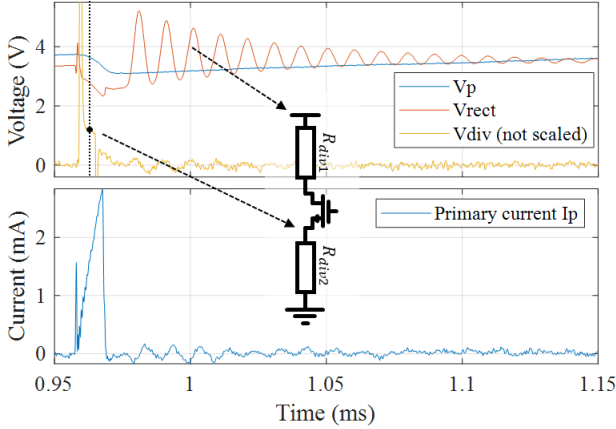


Figure 5 : Voltage and current measurements during the conduction of the flyback converter (zoom)

The MCU performs the voltage measurements thanks to its internal 12-bits ADC. The measured voltage is reduced to stay below the reference voltage of the ADC with a controlled voltage divider composed of 2 resistors and a NMOS (PMV88ENEA) to reduce power consumption (see Fig. 1 and 5). We see that the voltage divider is enabled during the first conduction stage and that the voltage is proportional to V_{rect} .

EXPERIMENTAL TEST BENCH

The operation and performances of our algorithm was validated by means of a DS1103 measurement system (dSPACE) coupled with Matlab (see Fig. 1). This acquisition system was used to measure different signals or receive them via an UART bus : V_p , V_{rect} , A_{in} (through V_{acc}) V_{div} , Φ , ... The current on V_{store} is measured with a N6705B DC Power Analyzer. This way we can measure the power P_{store} and thus the efficiency of the flyback converter. The experimental setup consists of an electromagnetic shaker controlled by an amplified dSPACE output into an acceleration. The output acceleration (fixed) is controlled with an internal regulation loop with an ICP accelerometer (352C68) as input. The PEH used in this paper is similar to the ones used in [12], its characteristics are given in Table 1. These characteristics are obtained when we fit a linear model to the results of the PEH with resistive loads.

Piezoelectric capacitance (C_p)	25 nF
Effective mass (M)	99 g
Short-circuit resonant frequency (f_{sc})	24.55 Hz
Spring constant (K)	2357 N/m
Damping coefficient (D)	254 mN/m/s
Electromechanical coupling coeff. (k_m^2)	4.7 %
Acceleration amplitude for tests (a)	0.2 m/s ²

Table 1 : Characteristics of the used PEH

We performed two different experiments in this paper. For the first experiment, the dSpace controlled a discrete programmable resistive load connected to the output of the rectifier. The voltage/phase measurements were performed by the dSpace system for different loads and input frequencies. The second experiment is identical except that the load was emulated with the DC/DC converter.

For both experiments, we first calculate the power $P(F, R) = \frac{V(F, R)^2}{R}$ with $V(F, R)$ being the different 3d maps of measured voltages (V_{rect} , V_{div} , ...). Once the powers are calculated, we can extract the optimal powers and load for each frequency. Then, the optimal resistive load is calculated (what the MPPT would have found) according to Eq. (1). As a first approach, the two emulated loads R_1 and R_2 were fixed to 100 k Ω and 1 M Ω .

RESULTS

Fig. 6 and Fig. 7 show the voltage and phase measurement respectively, received from the MCU.

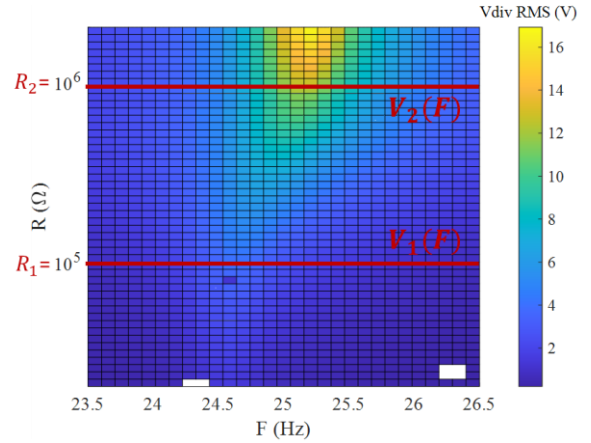


Figure 6 : RMS voltage measurements with the MCU of the signal V_{div} , sent to dSPACE/Matlab

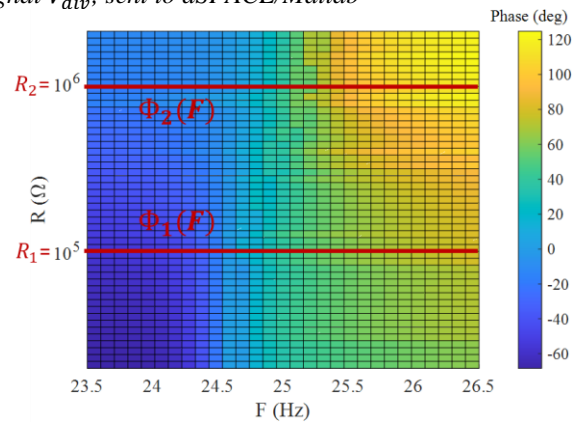


Figure 7 : Phase Φ between V_p and V_{rect} , measure with dSpace at the output of the comparators

Fig. 8 and 9 show the results of the method in terms of harvestable power (P_{rect}) and resistive load. On both figures, the line P_{max} in black corresponds to the theoretical maximum powers or optimal load.

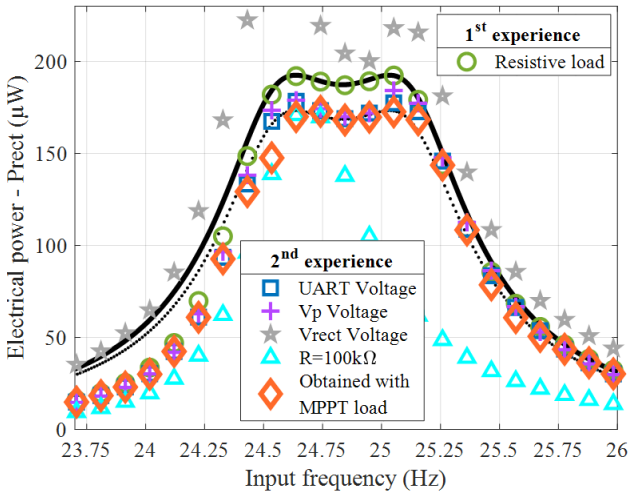


Figure 8 : Maximum and MPPT output powers

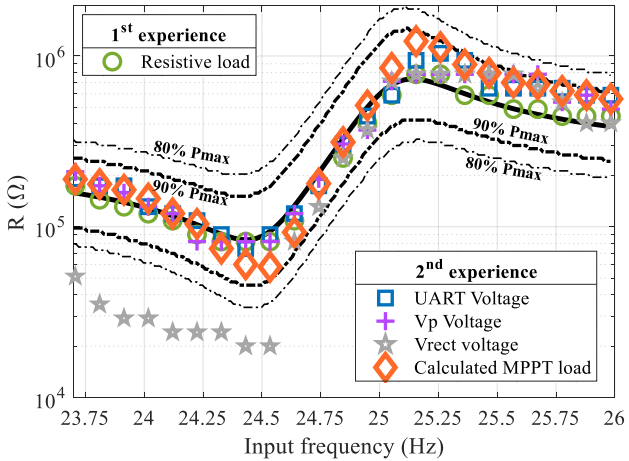


Figure 9 : Optimal and MPPT loads

The MPPT method gives a load that is close to the optimal load with the DC/DC converter and the associated power is in the 90% range of the optimal power. There is a small gap between the power obtained with resistive load and the one with the DC/DC converter. This gap will be investigated in future work.

We can clearly see here that the power obtained with measurements directly on V_{rect} is wrong compared to the power obtained with voltage information from the MCU. It justifies the measurement while the flyback converter is conducting with a NMOS controlled voltage divider.

Fig. 8 also shows the poor extraction performances if a fixed resistive load was applied to the PEH. This highlights the use of a MPPT algorithm and its implementation, even for moderately coupled PEH.

Finally, The consumption of the whole system has been measured when the MCU is in STOP2 mode (when it only emulates R_{opt}). In this configuration, only the comparators, the 100 kHz clock and the low-power timer were powered. We measured a current of $12.3\mu\text{A}$ (1.8V) when the emulated load is 20 kΩ and a current of $7.9\mu\text{A}$

(1.8V) when the emulated load is 200 kΩ. It corresponds to $22.1\mu\text{W}$ and $14.2\mu\text{W}$ respectively. The obtained electrical efficiency of the flyback converter is estimated to approximately 90%.

CONCLUSION

We have seen in this paper the implementation of a MPPT algorithm that calculates the optimal load with a low-power implementation and that finds the optimal impedance after a few mechanical cycles. The algorithm and load emulation consumes a maximum of $22\mu\text{W}$ when the optimal resistive load is emulated.

In this work, only the optimal resistive load is emulated to the PEH. Emulation of resistive and capacitive loads is planned for the following of this work with a higher coupling coefficient PEH. A low-power implementation of the measurement part of the algorithm is also planned for future work.

REFERENCES

- [1] Brenes et al., "Maximum Power Point of Piezoelectric Energy Harvesters."
- [2] Morel et al., "Short Circuit Synchronous Electric Charge Extraction (SC-SECE) Strategy for Wideband Vibration Energy Harvesting."
- [3] Brenes et al., "Large-Bandwidth Piezoelectric Energy Harvesting with Frequency-Tuning Synchronized Electric Charge Extraction."
- [4] Gibus et al. (in press), "High performance piezoelectric vibration energy harvesting by electrical resonant frequency tuning."
- [5] R. D'hulst, T. Sterken, R. Puers, G. Deconinck, and J. Driesen, "Power Processing Circuits for Piezoelectric Vibration-Based Energy Harvesters,"
- [6] Cai and Manoli, "A Piezoelectric Energy-Harvesting Interface Circuit with Fully Autonomous Conjugate Impedance Matching, 156% Extended Bandwidth, and $0.38\mu\text{W}$ Power Consumption."
- [7] Costanzo, Schiavo, and Vitelli, "Active Interface for Piezoelectric Harvesters Based on Multi-Variable Maximum Power Point Tracking."
- [8] Morel et al., "32.2 Self-Tunable Phase-Shifted SECE Piezoelectric Energy-Harvesting IC with a 30nW MPPT Achieving 446% Energy-Bandwidth Improvement and 94% Efficiency."
- [9] Çiftci et al., "A Low-Profile Autonomous Interface Circuit for Piezoelectric Micro-Power Generators."
- [10] Freychet et al., "Efficient Optimal Load and Maximum Output Power Determination for Linear Vibration Energy Harvesters with a Two-Measurement Characterization Method."
- [11] Decroix, Gasnier, and Badel, "An Efficient Maximum Power Point Tracking Architecture for Weakly Coupled Piezoelectric Harvesters Based on the Source I-V Curve."
- [12] Gibus, "Conception de Dispositifs Piézoélectriques Fortement Couplés Pour La Récupération d'énergie Vibratoire Large Bande."

CONTACT

*N. Decroix, tel: +33438781869; nicolas.decroix@cea.fr